**Title**

Sodium *myo*-inositol cotransporter-1, SMIT1, promotes cardiac hypertrophy and fibrosis in pressure overloaded mouse hearts.

**Authors**

Alice Marino[1,*], Julien Cumps[1], Laura Guilbert[1], Claire Baufays[1,2], Audrey Ginion[1], Laura Ferté[1], Sylvain Battault[1], Jerome Ambroise[3], Bertrand Bearzatto[3], Coert J. Zuurbier[4], Frank Lezoualch[5,6], Camille Pestiaux[7,8], Grzegorz Pyka[7,8], Greet Kerckhofs[7,8,9,10], Donatienne Tyteca[11], Caroline Bouzin[12], Luc Bertrand[1,13], Sandrine Horman[1], Christophe Beauloye[1,2,*].

**Affiliations**

[1] Pôle de Recherche Cardiovasculaire, Institut de Recherche Expérimentale et Clinique, Université catholique de Louvain, Brussels, Belgium

[2] Division of Cardiology, Cliniques Universitaires Saint-Luc, Université catholique de Louvain, Brussels, Belgium

[3] Centre de technologies moléculaires appliquées, Institut de Recherche Expérimentale et Clinique, Université catholique de Louvain, Brussels, Belgium

[4] Department of Anesthesiology, Amsterdam Cardiovascular Sciences, Amsterdam UMC, University of Amsterdam, the Netherlands

[5] Institut des Maladies Métaboliques et Cardiovasculaires, UMR-1297 Inserm, Université de Toulouse, Toulouse, France

[6] Université Toulouse, France Université Toulouse III-Paul Sabatier, Toulouse, France

[7] Mechatronic, Electrical Energy and Dynamic Systems, Institute of Mechanics, Materials and Civil Engineering, Université catholique de Louvain, Louvain-la-Neuve, Belgium

[8] Pole of Morphology, Institute of Experimental and Clinical Research, Université catholique de Louvain, Brussels, Belgium

[9] Department of Materials Engineering, KU Leuven, Heverlee, Belgium

[10] Prometheus, Division for Skeletal Tissue Engineering, KU Leuven, Leuven, Belgium

[11] CELL Unit, de Duve Institute and Université catholique de Louvain, Brussels, Belgium

[12] IREC Imaging Platform (2IP, RRID:SCR_023378), Institut de Recherche Expérimentale et Clinique, Université catholique de Louvain, Brussels, Belgium

[13] WELBIO Department, WEL Research Institute, Wavre, Belgium

**Short Title**

SMIT1 promotes cardiac hypertrophy.

**Corresponding authors**

Christophe Beauloye, E-mail: christophe.beauloye@uclouvain.be

Pôle de Recherche Cardiovasculaire, Institut de Recherche Expérimentale et Clinique, Université catholique de Louvain - Division of Cardiology, Cliniques Universitaires Saint-Luc. Av. Hippocrate 55, 1200 Brussels, Belgium

Alice Marino, E-mail: alice.marino@uclouvain.be

Pôle de Recherche Cardiovasculaire, Institut de Recherche Expérimentale et Clinique, Université catholique de Louvain. Av. Hippocrate 55, 1200 Brussels, Belgium

**Total word count** 7822

**Abstract**

**Background:** Sodium *myo*-inositol cotransporter-1 (SMIT1) belongs to the sodium-glucose cotransporter (SGLT) family. SMIT1 is expressed in cardiac cells, including fibroblasts and cardiomyocytes. However, the function of SMIT1 in the heart remains unknown.

**Methods:** We used a model of pressure overload induced by transverse aortic constriction in wild type (WT) mice and mice lacking SMIT1 (*Smit1*$^{-/-}$), combined with echocardiography, immunoblot and staining, contrast-enhanced microfocus computed tomography, and RNA-sequencing to evaluate the contribution of SMIT1 in cardiac hypertrophy, fibrosis and function. In addition, we used primary cultures of adult mouse and neonatal rat cardiomyocytes to define the molecular pathways affected by SMIT1.

**Results:** We found that aortic banding fails to induce systolic dysfunction, cardiac hypertrophy and fibrosis in *Smit1*$^{-/-}$ mice, in contrast to WT controls. Deletion of SMIT1 reduces cardiac *O*-GlcNAcylation and maintains basal levels of Carabin following hemodynamic stress. In the absence of SMIT1, Carabin inhibits calcineurin/NFAT and Ras/ERK1/2 pathways, putting a brake on transcriptional reprogramming and further development of cardiac hypertrophy. *In vitro*, we showed that the lack of SMIT1 mitigates phenylephrine-induced hypertrophy and calcium increase in isolated cardiomyocytes.

**Conclusions:** This work establishes SMIT1 as a key driver of hypertrophy, suggesting that pharmacological inhibition of this SGLT member can serve as a potential strategy to prevent or treat pathological hypertrophy and heart failure.

**Keywords**

Hypertrophy; Sodium *myo*-inositol cotransporter-1; Pressure overload; *O*-GlcNAcylation; Calcium fluxes

**Abbreviations**

| | |
|---|---|
| CaM | Calmodulin |
| CECT | Contrast-enhancing X-ray microfocus computed tomography |
| GO | Gene ontology |
| LV | Left ventricle |
| NButGT | 1,2-dideoxy-2′-propyl-alpha-d-glucopyranoso-[2,1-D]-Delta 2′-thiazoline |
| NFAT | Nuclear factor of activated T-cell |
| OGA | β-N-acetylglucosaminidase |
| *O*-GlcNAc | *O*-linked β-*N*-acetylglucosamine |
| OGT | *O*-GlcNAc transferase |
| ORA | Over Representation Analysis |
| PCA | Principal component analysis |
| PE | Phenylephrine |
| SGLT | Sodium-glucose cotransporter |
| SGLT2i | Sodium-glucose co-transporter-2 inhibitors |
| siRNA | Small interfering RNA |
| SMIT1 | Sodium *Myo*-inositol cotransporter-1 |
| *Smit1*$^{-/-}$ | SMIT1-deficient mice |
| TAC | Transverse aortic constriction |
| WT | Wild type |

## Introduction

Heart failure is a major healthcare problem associated with high hospitalization, morbidity and mortality[1]. It can result from chronic pathophysiological hemodynamic stresses, including pressure or volume overload. To adapt, the myocardium initiates compensatory mechanisms, such as cardiac hypertrophy, which become maladaptive and deleterious when sustained, ultimately leading to left ventricular dysfunction and heart failure. In response to pressure overload, increased intracellular calcium levels in cardiomyocytes initiates a signaling cascade that leads to activation of calmodulin (CaM)/calcineurin[2,3] and the subsequent nuclear translocation of nuclear factor of activated T-cell (NFAT)[2,4], promoting transcription factors and expression of hypertrophic genes[3]. Besides, the hexosamine biosynthetic pathway, which reversibly adds *O*-linked β-*N*-acetylglucosamine (*O*-GlcNAc) on protein Ser/Thr residues, has been shown to play an important role in the development of cardiac hypertrophy following hemodynamic stress[5,6].

Sodium-glucose cotransporters (SGLTs) comprehend seven plasma membrane proteins, each having a preferential sugar substrate that is transported using a downhill sodium gradient. Two SGLTs, SMIT1 and SGLT1, have been reported to be expressed in the heart[7,8]. However, SMIT1 is the only functional glucose transporter of the SGLT family[8], being expressed in cardiomyocytes[7], cardiac fibroblasts, endothelial, vascular smooth muscle[9], and inflammatory cells[10,11]. In hyperglycemic cardiomyocytes, SMIT1 acts as a glucose sensor and plays a major role in cardiac glucotoxicity, by activating NOX2 and increasing ROS production[7]. Hence, SMIT1 might be implicated in the pathophysiology of diabetic cardiomyopathy.

Although SMIT1 transports glucose with low affinity, its preferential substrate is *myo*-inositol ($K_m$=0.017 mM for *myo*-inositol and $K_m$=24 mM for glucose)[12,13]. The intracellular role of *myo*-inositol has been largely described, since it is a precursor of phosphoinositides and phosphatidyl inositols[14], essential molecules for calcium signaling, cell growth and survival[15,16]. However, the function of SMIT1 in the heart remains unclear.

Here we determined the impact of SMIT1 on cardiac function during the development of left ventricular remodeling and heart failure in an experimental mouse model of myocardial pressure overload induced by transverse aortic constriction (TAC). We found that the absence of SMIT1 protects the heart against pressure overload-induced fibrosis and hypertrophy by reducing cardiac *O*-GlcNAcylation and by blunting intracellular calcium dynamics and the consequent signaling cascade. This work identifies the SGLT member SMIT1 as an essential driver of the maladaptive response of the heart to hemodynamic stress, providing a potential therapeutic target to prevent pathological cardiac hypertrophy, left ventricular remodeling and the progression towards heart failure.

## Methods

### Animal handling

Animal handling and experimental procedures were approved by the local authorities (Comité d'éthique facultaire pour l'expérimentation animale, 2021/UCL/MD/009) and performed in accordance with the Guide for the Care and Use of Laboratory Animals, published by the US National Institutes of Health (NIH Publication, revised 2011). All animals were housed with a 12-h/12-h light/dark cycle, with the dark cycle occurring from 6.00 p.m. to 6.00 a.m. Mice were observed daily, and had free access to water and standard chow. SMIT1-deficient mice (*Smit1*$^{-/-}$) were generated as described elsewhere[17] and kindly donated to our laboratory. WT littermates were used as controls.

### Minimally invasive TAC

WT C57BL/6J and *Smit1*$^{-/-}$ mice (males and females, 12-14 weeks of age; body weight 19-23 g) were subjected to TAC or sham operation. More details can be found in the Supplemental Material.

### Echocardiographic analysis

Cardiac dimensions and function were analyzed by transthoracic echocardiography using a Vevo 3100 Imaging System (FUJIFILM VisualSonics, Toronto, Canada). All measurements and analysis were performed by the same experienced operator who was blinded to the experimental groups using VevoLab 5.5.1 software. Successful TAC surgery was determined 3 days after surgery by an aortic peak velocity measured by echo

Doppler: mice were included in the study when peak velocity was ≥ 2500 mm/s. More details can be found in the Supplemental Material.

**Assessment of cross-sectional cardiomyocytes area with WGA staining**

Heart sections were routinely stained with wheat germ agglutinin (WGA) to determine cardiomyocyte size. Cardiomyocyte size was analyzed among the entire LV wall of base and middle areas (~500 cardiomyocytes per animal), using Axiovision software (Carl Zeiss). Details can be found in the Supplemental Material.

**Assessment of cardiac fibrosis with Picrosirius red staining**

Paraffine embedded heart sections were stained with picrosirius red solution. Myocardial fibrosis was analyzed on four to eight heart sections per animal using Visiopharm software. Fibrosis was quantified as percentage of picrosirius red stained area relative to total area of interest (LV area). Details can be found in the Supplemental Material.

**Quantitative analysis of hypertrophy in isolated cardiomyocytes**

Coverslips with either adult mouse or neonatal rat cardiomyocytes were incubated 1h with anti-α-actinin antibody (A7811, Sigma) at room temperature, followed with incubation with anti-mouse secondary antibody coupled to Alexa fluor 594. Cell size (>100 cells per samples) was determined using AxioVision software (Carl Zeiss). Details can be found in the Supplemental Material.

### Contrast-enhancing X-ray microfocus computed tomography (CECT)

After fixation in PFA 4%, murine hearts underwent contrast-enhanced microCT (CECT) imaging. Fibrotic areas, having a different grey value compared to the healthy tissue, were manually segmented using CTan software (Bruker MicroCT, Kontich, Belgium). Details can be found in the Supplemental Material.

### NFAT-luciferase assay

Luciferase activity was measured in supernatants with Luciferase Assay System (LAR, E1500, Promega) following manufacturer's instruction. Briefly, 20 µl of cell lysate was added to 100 µl of LAR. Luminescence was measured immediately after with PerkinElmer Victor plate reader. Details can be found in the Supplemental Material.

### Immunoblotting analysis

Lysates of sham- and TAC-operated hearts and isolated cardiomyocytes were used for Western Blots. Details can be found in the Supplemental Material.

### RNA extraction and mRNA expression

Total RNA was isolated from mouse LV using the Qiagen RNeasy Mini Kit for mRNA analyses (Qiagen, 74106). List of oligos is accessible and details can be found in the Supplemental Material.

## RNA sequencing

Total RNA was isolated from the LV of five WT and five *Smit1*$^{-/-}$ mice at baseline and at two weeks after TAC surgery, and treated with DNase according to the manufacturer's instructions. Raw and processed RNA-seq data were deposited and made publicly available on the Gene Expression Omnibus (GSE245135). Details can be found in the Supplemental Material.

## Intracellular calcium measurements in adult mouse cardiomyocytes

Calcium fluxes were measured with the fluorescent calcium indicator fluo-4-AM (F14201, ThermoFisher) in adult mouse cardiomyocytes isolated from WT and *Smit1*$^{-/-}$ mice. Additional details can be found in the Supplemental Material.

## Statistics

The data are presented as means ± SEM from at least 4 independent experiments. Statistical significance was determined with 2-way ANOVA followed by Kruskal-Wallis post-hoc test or unpaired Student t-test using GraphPad Prism software (9.1.2 version).

## Results

### The absence of SMIT1 protects against left ventricular remodeling induced by pressure overload.

We previously showed that the absence of SMIT1 affects neither cardiac morphology nor function under basal state[7]. This is stable over time, since 1-year-old *Smit1*$^{-/-}$ mice do not show altered cardiac function, fibrosis and hypertrophy, or changes in plasma *myo*-inositol levels compared to the wild type (WT) (Figure S1, Table S1). However, RNAseq analysis from WT and *Smit1*$^{-/-}$ hearts at baseline highlighted differentially expressed genes involved in cardiac fibrosis, hypertrophy, and function (Figure S1a-k), suggesting that SMIT1 may be implicated in left ventricular (LV) remodeling.

To establish the contribution of SMIT1 in pathological cardiac remodeling, we subjected WT and *Smit1*$^{-/-}$ mice for two weeks to hemodynamic stress induced by TAC surgery. Three days after TAC, aortic peak velocity was evaluated by echo Doppler to confirm a successful aortic banding, which revealed a similar massive pressure overload in both strains (Figure S2a,b). TAC surgery led to an increase in *Smit1* mRNA expression in WT mice, while it remained undetectable in both sham- and TAC-operated *Smit1*$^{-/-}$ mouse hearts (Figure S2c). Notably, plasmatic levels of *myo*-inositol were not changed by the surgery and between the two genotypes (Figure S2d).

Two weeks post-TAC, echocardiographic analysis of WT mouse hearts showed a significant increase in LV mass associated with a reduced systolic function (reduced ejection fraction, fractional shortening, and increased LV end-systolic volume and internal dimension) compared to their sham controls (Figure 1a-d, and Table S2). In contrast,

*Smit1*$^{-/-}$ mice were protected from TAC-induced adverse LV remodeling (Figure 1a-d), indicating a higher tolerance to pressure overload.

In addition, histological analysis showed a significant increase in the cross-sectional area of LV cardiomyocytes (Figure 1e,f), and in collagen deposition (Figure 1g,h) in TAC-operated WT but not *Smit1*$^{-/-}$ mice. Similar results were obtained in WT and *Smit1*$^{-/-}$ mice treated with Ang II subcutaneous infusion, an alternative approach to induce pressure overload (Figure S2e-h). RT-qPCR analysis revealed that the expression of pro-fibrotic markers (*Col1a* and *α-SMA*) was increased in WT mouse hearts, compared to *Smit1*$^{-/-}$ two weeks after TAC (Figure 1i). Post-mortem analysis also revealed an increased heart weight-tibia length ratio in WT animals after TAC surgery, which was markedly blunted in *Smit1*$^{-/-}$ (Figure 1j). Finally, contrast-enhanced microfocus computed tomography (CECT) analysis demonstrated that heart and fibrotic volumes were less pronounced in TAC-operated *Smit1*$^{-/-}$ mutants compared to WT mice (Figure 1k, Videos S1-S2). Hence, SMIT1 drives maladaptive cardiac hypertrophy and fibrosis following pressure overload.

**SMIT1 aggravates cardiac hypertrophy by increasing protein *O*-GlcNAcylation.**

*O*-GlcNAcylation globally increases with cardiac pressure overload and contributes to cardiac hypertrophy[5,6]. To assess whether the impact of SMIT1 on cardiac hypertrophy involves *O*-GlcNAcylation, we performed immunoblotting analysis using heart lysates from WT and *Smit1*$^{-/-}$ mice two weeks after TAC or sham surgery. As expected, the levels of *O*-GlcNAcylated proteins were elevated in WT TAC-operated heart lysates compared to sham (Figure 2a,b). In contrast, *Smit1*$^{-/-}$ heart lysates showed

reduced protein *O*-GlcNAcylation compared to WT (Figure 2a,b). This was associated with a reduced expression of *O*-GlcNAc transferase (OGT) in TAC-operated *Smit1*$^{-/-}$ mice (Figure 2c), suggesting that the absence of SMIT1 protects against pressure overload-induced hypertrophy through reduced OGT expression and *O*-GlcNAcylation. Moreover, following aortic banding, AMPK activation, a key regulator of *O*-GlcNAcylation, was not altered by SMIT1 deficiency (data not shown).

We next examined the direct effect of SMIT1 on hypertrophy of isolated cardiomyocytes from adult WT and *Smit1*$^{-/-}$ mice. Treatment with the pro-hypertrophic agent phenylephrine (PE, 50 µM) led to an increase in the size of cardiomyocytes isolated from WT, but not from *Smit1*$^{-/-}$ mouse hearts (Figure 2d,e). In addition, PE treatment augmented *O*-GlcNAcylation in WT cardiomyocytes, but not in *Smit1*$^{-/-}$ cells (Figure 2f,g). Similarly, neonatal rat cardiomyocytes transfected with scramble small interfering RNA (siRNA) showed a significant increase in size and protein *O*-GlcNAcylation following treatment with PE (20 µM). However, a 3-fold reduction of SMIT1 expression using SMIT1-specific siRNA (Figure S3a) prevented PE-induced increase in cardiomyocyte size and protein *O*-GlcNAcylation (Figure 2h-k). Hence, SMIT1 aggravates cardiac hypertrophy through the induction of protein *O*-GlcNAcylation.

To test whether the impact of SMIT1 on cardiac hypertrophy is indeed caused by *O*-GlcNAcylation, we promoted *O*-GlcNAcylation using two β-N-acetylglucosaminidase (OGA) inhibitors Thiamet G and 1,2-dideoxy-2′-propyl-alpha-d-glucopyranoso-[2,1-D]-Delta 2′-thiazoline (NButGT, Figure 3a). In cardiomyocytes isolated from WT and *Smit1*$^{-/-}$ mice, Thiamet G treatment (30 nM) strongly increased basal *O*-GlcNAcylation levels (Figure 3b, and Figure S3b), but was not sufficient to induce an increase in cell size

(Figure 3c,d). This confirms that increased *O*-GlcNAcylation alone is necessary but not sufficient to promote cardiac hypertrophy[5]. However, co-treatment with PE and Thiamet G increased cardiomyocytes size in both WT and *Smit1*$^{-/-}$ (Figure 3c,d), demonstrating that pharmacological induction of *O*-GlcNAcylation counteracts the protection conferred by the absence of SMIT1.

Next, we tested whether this was also the case *in vivo*. We injected TAC-operated WT and *Smit1*$^{-/-}$ mice with the OGA inhibitor NButGT (50 mg/kg) every day for two weeks (Figure 3e and Figure S3c). NButGT treatment markedly increased *O*-GlcNAcylation levels in *Smit1*$^{-/-}$ mouse hearts (Figure 3f,g), and abolished the differences in LV mass (Figure S3d) and cardiomyocyte size between WT and *Smit1*$^{-/-}$ hearts following pressure overload (Figure 3h,j). In TAC-operated WT mice, NButGT induced a partial reduction of LV mass and cardiomyocyte size (Figure 3h,j, and Figure S3d,e).

However, following NButGT treatment, a modest improvement of systolic function was still observed in TAC-operated *Smit1*$^{-/-}$ mice, compared to WT (Figure S3f,g), suggesting that alternative pathways may be involved downstream of SMIT1, in addition to *O*-GlcNAcylation. This hypothesis is further supported by the inability of NButGT to impact cardiac fibrosis (Figure 3i,k).

**Transcriptomic analysis reveals Carabin as a putative target of SMIT1-induced cardiac hypertrophy.**

To identify the pathways affected by SMIT1, we performed myocardial transcriptomic analysis in five WT and five *Smit1*$^{-/-}$ mouse hearts two weeks following TAC. A principal component analysis (PCA) was performed to distinguish the

transcriptomic profiles of WT from *Smit1*$^{-/-}$ hearts and revealed a distinct separation between the two genotypes (Figure 4a). RNA-seq identified 14593 genes, of which 254 (1.7%) were differentially expressed (fold change ≥ 2 and FDR <0.05) (Figure 4b, and Table S3). Significant modulations were found for many genes involved in hypertrophy, fibrosis and cardiac contractility (Figure 4c). Furthermore, Over Representation Analysis (ORA) analysis identified many enriched gene ontologies (GO) terms among which several biological processes (BP) related to extracellular matrix organization, cell differentiation and development, as well as regulation of ion transport (Figure 4d).

Among these genes, Carabin (alias *Tbc1d10c*) was significantly upregulated in *Smit1*$^{-/-}$ mice compared to WT animals (Figure 4b,c). Carabin is an endogenous inhibitor of calcineurin/NFAT and Ras/ERK1/2 pathways[2,28], highly expressed in the immune system[29,30], but also present in the heart where it exerts antihypertrophic effects[2]. Calcineurin/NFAT and Ras/ERK1/2 pathways are negatively regulated through two distinct domains of Carabin, ultimately putting a brake on transcriptional reprogramming and development of cardiac hypertrophy[28,29]. While TAC surgery leads to downregulation of Carabin expression in WT mice, Carabin expression is preserved in TAC-operated *Smit1*$^{-/-}$ mutants (Figure 5a). First, this elicits a decreased expression of *Rcan1.4*, a readout for calcineurin activity[31] (Figure 5b), and the hypertrophic markers atrial natriuretic peptide (*Nppa*) and brain natriuretic peptide (*Nppb*) (Figure 5c). Second, ERK phosphorylation was strongly decreased in TAC-operated *Smit1*$^{-/-}$ mice compared to WT mice (Figure 5d,e). Accordingly, Carabin mRNA levels were inversely correlated with cardiomyocyte area, suggesting that high Carabin expression translates into reduced cardiomyocyte size (Figure 5f).

We next addressed whether SMIT1 impacts Carabin-dependent NFAT signaling pathway in neonatal rat ventricular cardiomyocytes. We found that PE treatment potentiated NFAT nuclear translocation in cells transfected with control siRNA, but not with *Smit1*-specific siRNA (Figure 5g).

To verify that this depends on Carabin, we double-transfected neonatal rat cardiomyocytes with a combination of si*Smit1* and si*Carabin*, which induced a significant downregulation of mRNA expression of SMIT1 and Carabin (Figure S4a,b). Following treatment with PE (20 µM), the protective effect observed in si*Smit1* knockdown on cardiomyocyte surface area was abolished in the double si*Smit1* + si*Carabin* knockdown, as well as when Carabin alone was downregulated (Figure 5h,i). Therefore, the lack of SMIT1 elicits sufficient Carabin levels to put a brake on calcineurin activity, NFAT translocation and promotion of pro-hypertrophic gene transcription factors, ERK phosphorylation, ultimately protecting the heart against stress-induced cardiac hypertrophy.

Finally, we assessed *O*-GlcNAcylation in cells with SMIT1 and Carabin downregulation. Surprisingly, we found that Carabin knockdown prevented the increase of protein *O*-GlcNAcylation following PE treatment to the same extent when concomitant knockdown of SMIT1 and Carabin occurred (Figure 5j,k). This demonstrates that downregulation of Carabin during hypertrophy is not responsible for the increase of *O*-GlcNAcylation.

**The absence of SMIT1 attenuates PE-induced calcium fluxes in cardiomyocytes.**

Cardiac hypertrophy develops in response to abnormalities in calcium handling[32]. PE induces intracellular calcium overload, which regulates several calcium-dependent proteins, such as calcineurin, activating gene reprogramming and pro-hypertrophic signaling pathways[33].

We tested whether SMIT1 impacts cardiac hypertrophy via alteration of cardiomyocyte calcium dynamics in response to PE. Cardiomyocytes isolated from WT and *Smit1*$^{-/-}$ mice were loaded with Fluo-4, then treated with PE (50 µM), and calcium fluxes were recorded over time in living cells. In WT cardiomyocytes, PE treatment increased the intensity of calcium fluxes about two-fold, while the lack of SMIT1 completely prevented this increase (Figure 6a-c, Videos S3-6). Interestingly, we also found that *myo*-inositol directly increases sodium and calcium concentrations (Figure S5a-c). Altogether, these data show that SMIT1 controls cardiac hypertrophy by altering the ionic fluxes in response to PE.

Finally, we found that PE treatment leads to increased Carabin levels in WT cardiomyocytes, in agreement with previous findings[2], and that the deletion of SMIT1 promotes Carabin expression in a calcium-independent manner (Figure 6d). Thus, the decrease in Carabin expression observed in mice subjected to pressure overload is unlikely to be caused by changes in calcium levels.

## Discussion

Here, we established the impact of SMIT1 in the development of cardiac hypertrophy, fibrosis, and dysfunction, and its downstream signaling in murine hearts subjected to pressure overload. We demonstrated that SMIT1 modulates cardiac hypertrophy by three distinct mechanisms: (i) increased *O*-GlcNAcylation, (ii) reduced Carabin expression, and (iii) enhanced calcium-dependent transcriptional reprogramming (graphical abstract).

### SMIT1 affects *O*-GlcNAcylation in pressure overload-induced cardiac hypertrophy

We and others previously identified increased *O*-GlcNAcylation as a dynamic effector of cardiac hypertrophy following pressure overload[5,6,34]. Under these circumstances, cardiac *O*-GlcNAc levels are not primarily regulated by glucose availability, which remains unchanged, but rather controlled by the three key enzymes of the hexosamine biosynthetic pathway (GFAT, OGT, and OGA)[5,6,35-37]. Indeed, activation of AMPK decreases GFAT activity, OGT expression and *O*-GlcNAc levels in aortic banded heart[5]. Here we show that the lack of SMIT1 counteracts pressure overload-induced *O*-GlcNAcylation most likely by attenuating OGT expression, thus reducing cardiac hypertrophy. We currently do not know how SMIT1 regulates OGT expression. A direct link between *myo*-inositol and AMPK activation recently emerged[38], suggesting that SMIT1 may be involved in AMPK-dependent signaling. However, this seems unlikely considering that we did not observe different AMPK activation in TAC-operated WT and *Smit1*$^{-/-}$ mouse hearts.

How pressure overload controls *O*-GlcNAcylation remains a complex matter which is not fully understood. More than 200 proteins with changes in *O*-GlcNAcylation levels have been identified during cardiac hypertrophic remodeling[39], although the functional relevance of these modifications have for the most part not been established. It has been shown that *O*-GlcNAcylation of CaMKII on Ser280 increases cardiomyocyte size, activates NOX2, with consequent ROS production and exacerbation of hyperglycemic cardiomyocytes pathological state[40-43]. Cardiac Troponin I and myosin light chain 2 can also be *O*-GlcNAcylated at Ser150 and Ser15, respectively, and change the cardiac phenotype by decreasing calcium sensitivity and cardiac contractility[44]. It will be of high interest to identify *O*-GlcNAcylated proteins downstream of SMIT1 to better define the pathways driving cardiac hypertrophy, including those ones involved in ROS-producing machinery and calcium sensitivity.

We used OGA inhibitors, *in vivo* and *in vitro*, to increase *O*-GlcNAcylation, and found that NButGT not only failed to fully block the anti-hypertrophic action of SMIT1 deletion, but had no impact on cardiac fibrosis, corroborating the hypothesis that *O*-GlcNAcylation is not the only mechanism downstream SMIT1.

**SMIT1 regulates ion exchanges**

Aberrant transmembrane calcium fluxes, leading to intracellular calcium overload are the most common hypertrophic triggers[32]. It has been shown that SMIT1, by transporting *myo*-inositol intracellularly, plays a critical role in the production of PIP and $PIP_2$ and increases calcium release from intracellular stores[14]. Here, we show that PE induces an increase in calcium fluxes in cardiomyocytes, and that this effect is blunted in

the absence of SMIT1. Moreover, *myo*-inositol also increases the intracellular concentration of sodium and calcium in adult rat cardiomyocytes. Our hypothesis is that SMIT1, by co-transporting sodium and *myo*-inositol, plays a crucial role in ionic exchanges, impacting gene expression reprogramming and consequent cardiac hypertrophy. SMIT1 is located in close proximity of caveolae structures[7], where it could interact with other ion channels, such as sodium/calcium exchanger (NCX), or sodium/hydrogen exchanger (NHX), unbalancing the ionic downstream signaling[7,45].

Interestingly, *myo*-inositol levels are similar in WT and *Smit1*$^{-/-}$ mouse plasma, regardless of TAC surgery (Figure S1j), and present in cardiomyocyte culture medium. We speculate that in the presence of hypertrophic stimuli (TAC or PE), lack of SMIT1 protects against hypertrophy by attenuating intracellular ion dynamics. Presumably, the absence of SMIT1 alters the intracellular *myo*-inositol levels and the subsequent generation of its metabolites, including $PIP_2$ and $IP_3$. Further studies are needed to understand the contribution of *myo*-inositol/SMIT1 to cardiomyocytes calcium signaling and function.

**SMIT1 deletion protects against cardiac hypertrophy via the Carabin pathway**

We identified a novel pathway affected by SMIT1 expression which is involved in calcium signaling: *Tbc1d10c*, the gene encoding for Carabin. Carabin prevents cardiac hypertrophy through its negative action on calcineurin/NFAT, Ras/ERK and CaMKII signaling pathways[2]. In cardiac samples of patients with heart failure and in WT TAC-operated mice, Carabin is downregulated, favoring hypertrophic signaling, while its overexpression limits hypertrophic remodeling[2]. Here we found that Carabin mRNA

expression is preserved in TAC-operated *Smit1*$^{-/-}$ mice, thereby decreasing calcineurin activity, NFAT translocation, and hypertrophic genes (*Nppa*, *Nppb*). Downregulation of Carabin counteracts the effects of SMIT1 deletion on cardiomyocytes size, reinforcing the hypothesis that Carabin is the major mechanism governed by SMIT1 in cardiac hypertrophy.

We wondered whether SMIT1-dependent changes in Carabin expression were dictated by intracellular calcium levels. We and others[2] found that in WT isolated cardiomyocytes treated with PE, Carabin expression was elevated, most likely to counteract the early stage of hypertrophy. However, even without PE, the lack of SMIT1 led to a significant enhanced expression of Carabin. Collectively these data indicate that SMIT1 directly regulates Carabin expression, and that this role is independent from intracellular calcium.

We found that downregulation of Carabin reduces *O*-GlcNAcylation, despite the hypertrophic effect on cardiomyocytes. This is a newly identified role for Carabin. Since *O*-GlcNAcylation induces hypertrophic signaling via activation of calcium/calcineurin-NFAT mediated pathway[46], we speculate that increased NFAT translocation driven by downregulation of Carabin could work as a negative feedback loop to prevent further *O*-GlcNAcylation. Our study provides evidence that Carabin is modulated by a membrane protein, offering an easy target to prevent cardiac hypertrophy.

In addition to the classical pro-hypertrophic *Nppa*, *Nppb*, and *Acta1*, RNAseq showed several genes involved in cardiac hypertrophy to be significantly affected by the lack of SMIT1 (Table S3). Of note, *Ankrd1* and *Ankrd2* were significantly downregulated in TAC-operated *Smit1*$^{-/-}$ mice compared to WT. These genes encode for proteins that

finely mediate cardiomyocytes response to hemodynamic stress, and enhanced expression have been associated with the onset of cardiac hypertrophy and diastolic dysfunction[47-50]. Interestingly, an increase in ANKRD1 levels induces ERK phosphorylation with subsequent development of cardiac hypertrophy[49]. Thus, we speculate that ANKRD1 and 2 may be additional downstream effectors of SMIT1 that control the hypertrophic response.

**SMIT1 plays a role in cardiac fibrosis and may affect fibroblasts properties.**

In addition to cardiomyocytes, SMIT1 is also expressed in cardiac fibroblasts and might modulate the hypertrophic phenotype. Here, we used the innovative CECT analysis to visualize fibrosis spatial distribution along the myocardium in a 3D manner[51], which allowed us to perform micro-structural analysis of the entire heart. With this approach we measured the volume and the distribution of fibrotic areas in the whole WT and *Smit1*$^{-/-}$ mouse hearts and found that the lack of SMIT1 decreased cardiac fibrosis following aortic banding. Moreover, SMIT1 deletion led to a significant downregulation of major genes involved in extracellular matrix composition (Table S3), suggesting that SMIT1 may play a role in the regulation of cardiac fibroblast properties.

Given the interplay between cardiomyocytes and fibroblasts during left ventricular remodeling, it will be interesting to use cell-type specific conditional SMIT1 knockouts to delineate the contribution of cardiomyocytes and cardiac fibroblasts in SMIT1-induced development of heart failure.

**SMIT1 as a new potential target for the treatment of cardiac hypertrophy and heart failure**

Following TAC, SMIT1 expression is increased in murine hearts. In humans, polymorphisms at the *SLC5A3* locus, that result in increased SMIT1 expression, have been associated with high risk of cardiovascular diseases[52,53]. In addition, *myo*-inositol levels were found to be elevated in a small cohort of patients with advanced heart failure compared to healthy controls[54], highlighting the interest in preventing/inhibiting SMIT1 signaling.

Our results suggest that inhibition of SMIT1 signaling may represent an effective approach to prevent or treat heart failure, particularly since SMIT1 is expressed at the plasma membrane and is therefore an attractive pharmacological target. Recently, sodium-glucose co-transporter-2 inhibitors (SGLT2i - developed to treat type 2 diabetes) proved beneficial in patients with heart failure, regardless of the presence of type 2 diabetes, contributing to the restoration of cardiac metabolism reprogramming[55]. Yet, the mechanisms by which SGLT2i protect the heart from failing are still unclear and under investigation, given that SGLT2 is not expressed in the heart, at least under physiological conditions[56]. However, lowering of cytosolic sodium and calcium also figures prominently as an explanation of SGLT2i's protective effects[57], similarly as we now suggest for SMIT1 detrimental actions. One possibility is that the beneficial effect of SGLT2i in the heart may derive (at least partially) from SMIT1 inhibition. Nevertheless, SGLT2i plasma concentrations in patients do not reach the values for SMIT1 inhibition[58] ($IC_{50}$ of empagliflozin and dapagliflozin are estimated to be 8.3 and 22 μM, respectively)[59].

Collectively, our work provides important insights into the role of SMIT1 in the development of cardiac hypertrophy and progression to heart failure. These findings reveal SMIT1 as a new target to ameliorate cardiac contractile dysfunction.

**Acknowledgements**

We would like to thank Gerard Berry for kindly providing *Smit1*$^{-/-}$ mice, Benjamin Lauzier for synthetizing NButGT, Tim Balcaen and Prof. Wim De Borggraeve (KU Leuven) for the development and synthesis of Hf-WD 1:2 POM, and Prof. Roberto Levi for his contribution in revising the manuscript.

**Sources of Funding**

This work was supported by bilateral research programs between Fonds de Recherche du Quebec (FRQ, Québec, Canada) and Fonds National de la Recherche Scientifique (FRS-FNRS, Wallonia-Brussels Federation) (Bilateral research projects FRQ-FNRS - PINT-BILAT-P 2018). It was also funded by grants from the FRS-FNRS (T.0009.21, T.0007.23 and EQP - Tomo4D- U.N069.20), Action de Recherche Concertée de la Communauté Wallonie-Bruxelles, Belgium (ARC 18/23-094 and 19/24-097), SBO project of the Research Foundation Flanders (FWO; grant S007219N), ASBL Jean Degroof-Marcel Van Massenhove funding, and the UCLouvain Foundation Saint-Luc (RM2A project). Prof. Sandrine Horman works as senior research associate at FNRS, Belgium. Prof. Luc Bertrand is supported by a grant from Walloon Excellence Research Institute WELRI-WELBIO (Belgium).

**Disclosures**

None

## Novelty and Significance

### What Is Known?

- Sodium myo-inositol cotransporter-1, SMIT1, is the most expressed SGLT member in the murine heart.
- Increased SMIT1 expression has been associated with high risk of cardiovascular diseases in genome-wide association studies.

### What New Information Does This Article Contribute?

- Deletion of SMIT1 protects against the development of cardiac hypertrophy, fibrosis, and dysfunction in murine hearts subjected to pressure overload.
- The absence of SMIT1 reduces *O*-GlcNAcylation in mouse hearts and in isolated cardiomyocytes subjected to hypertrophic stimuli.
- SMIT1 deficiency attenuates calcium-dependent transcriptional reprogramming.

Cardiac hypertrophy and fibrosis contribute to the development of left ventricular remodeling and progression towards heart failure. Here, we show that the lack of SMIT1 protects against cardiac hypertrophy, fibrosis, and dysfunction in murine hearts subjected to pressure overload. We demonstrate that SMIT1 impinges on cardiac function through increased protein *O*-GlcNAcylation and calcium-dependent transcriptional reprogramming. Hence, pharmacological inhibition of this membrane transporter constitutes an attractive strategy for the prevention and/or treatment of heart failure.

## References


1. Savarese G, Becher PM, Lund LH, Seferovic P, Rosano GMC, Coats AJS. Global burden of heart failure: a comprehensive and updated review of epidemiology. *Cardiovascular research*. 2023;118:3272-3287. doi: 10.1093/cvr/cvac013
2. Bisserier M, Berthouze-Duquesnes M, Breckler M, Tortosa F, Fazal L, de Régibus A, Laurent AC, Varin A, Lucas A, Branchereau M, et al. Carabin protects against cardiac hypertrophy by blocking calcineurin, Ras, and Ca2+/calmodulin-dependent protein kinase II signaling. *Circulation*. 2015;131:390-400; discussion 400. doi: 10.1161/circulationaha.114.010686
3. Anderson ME, Brown JH, Bers DM. CaMKII in myocardial hypertrophy and heart failure. *J Mol Cell Cardiol*. 2011;51:468-473. doi: 10.1016/j.yjmcc.2011.01.012
4. MacDonnell SM, Weisser-Thomas J, Kubo H, Hanscome M, Liu Q, Jaleel N, Berretta R, Chen X, Brown JH, Sabri AK, et al. CaMKII negatively regulates calcineurin-NFAT signaling in cardiac myocytes. *Circ Res*. 2009;105:316-325. doi: 10.1161/circresaha.109.194035
5. Gelinas R, Mailleux F, Dontaine J, Bultot L, Demeulder B, Ginion A, Daskalopoulos EP, Esfahani H, Dubois-Deruy E, Lauzier B, et al. AMPK activation counteracts cardiac hypertrophy by reducing O-GlcNAcylation. *Nat Commun*. 2018;9:374. doi: 10.1038/s41467-017-02795-4
6. Lunde IG, Aronsen JM, Kvaløy H, Qvigstad E, Sjaastad I, Tønnessen T, Christensen G, Grønning-Wang LM, Carlson CR. Cardiac O-GlcNAc signaling is increased in hypertrophy and heart failure. *Physiol Genomics*. 2012;44:162-172. doi: 10.1152/physiolgenomics.00016.2011

7. Van Steenbergen A, Balteau M, Ginion A, Ferte L, Battault S, Ravenstein CM, Balligand JL, Daskalopoulos EP, Gilon P, Despa F, et al. Sodium-myoinositol cotransporter-1, SMIT1, mediates the production of reactive oxygen species induced by hyperglycemia in the heart. *Sci Rep*. 2017;7:41166. doi: 10.1038/srep41166

8. Ferté L, Marino A, Battault S, Bultot L, Van Steenbergen A, Bol A, Cumps J, Ginion A, Koepsell H, Dumoutier L, et al. New insight in understanding the contribution of SGLT1 in cardiac glucose uptake: evidence for a truncated form in mice and humans. *Am J Physiol Heart Circ Physiol*. 2021. doi: 10.1152/ajpheart.00736.2019

9. Barrese V, Stott JB, Baldwin SN, Mondejar-Parreño G, Greenwood IA. SMIT (Sodium-Myo-Inositol Transporter) 1 Regulates Arterial Contractility Through the Modulation of Vascular Kv7 Channels. *Arterioscler Thromb Vasc Biol*. 2020;40:2468-2480. doi: 10.1161/atvbaha.120.315096

10. De Paepe B, Merckx C, Jarošová J, Cannizzaro M, De Bleecker JL. Myo-Inositol Transporter SLC5A3 Associates with Degenerative Changes and Inflammation in Sporadic Inclusion Body Myositis. *Biomolecules*. 2020;10. doi: 10.3390/biom10040521

11. A single-cell transcriptomic atlas characterizes ageing tissues in the mouse. *Nature*. 2020;583:590-595. doi: 10.1038/s41586-020-2496-1

12. Wright EM. Glucose transport families SLC5 and SLC50. *Mol Aspects Med*. 2013;34:183-196. doi: 10.1016/j.mam.2012.11.002

13. Alfadda AA, Sallam RM. Reactive oxygen species in health and disease. *J Biomed Biotechnol*. 2012;2012:936486. doi: 10.1155/2012/936486

14. Dai G, Yu H, Kruse M, Traynor-Kaplan A, Hille B. Osmoregulatory inositol transporter SMIT1 modulates electrical activity by adjusting PI(4,5)P2 levels. *Proc Natl Acad Sci U S A*. 2016;113:E3290-3299. doi: 10.1073/pnas.1606348113

15. Croze ML, Soulage CO. Potential role and therapeutic interests of myo-inositol in metabolic diseases. *Biochimie*. 2013;95:1811-1827. doi: 10.1016/j.biochi.2013.05.011

16. Su XB, Ko AA, Saiardi A. Regulations of myo-inositol homeostasis: Mechanisms, implications, and perspectives. *Adv Biol Regul*. 2023;87:100921. doi: 10.1016/j.jbior.2022.100921

17. Berry GT, Wu S, Buccafusca R, Ren J, Gonzales LW, Ballard PL, Golden JA, Stevens MJ, Greer JJ. Loss of murine Na+/myo-inositol cotransporter leads to brain myo-inositol depletion and central apnea. *J Biol Chem*. 2003;278:18297-18302. doi: 10.1074/jbc.M213176200

18. Ginsberg AP. *Inorganic Syntheses, Volume 27*. John Wiley & Sons; 1991.

19. Orjuela S, Huang R, Hembach KM, Robinson MD, Soneson C. ARMOR: An Automated Reproducible MOdular Workflow for Preprocessing and Differential Analysis of RNA-seq Data. *G3 (Bethesda)*. 2019;9:2089-2096. doi: 10.1534/g3.119.400185

20. Patro R, Duggal G, Love MI, Irizarry RA, Kingsford C. Salmon provides fast and bias-aware quantification of transcript expression. *Nat Methods*. 2017;14:417-419. doi: 10.1038/nmeth.4197

21. Soneson C, Love MI, Robinson MD. Differential analyses for RNA-seq: transcript-level estimates improve gene-level inferences. *F1000Res*. 2015;4:1521. doi: 10.12688/f1000research.7563.2

22. Robinson MD, McCarthy DJ, Smyth GK. edgeR: a Bioconductor package for differential expression analysis of digital gene expression data. *Bioinformatics*. 2010;26:139-140. doi: 10.1093/bioinformatics/btp616

23. Liao Y, Wang J, Jaehnig EJ, Shi Z, Zhang B. WebGestalt 2019: gene set analysis toolkit with revamped UIs and APIs. *Nucleic Acids Res*. 2019;47:W199-w205. doi: 10.1093/nar/gkz401

24. Jassal B, Matthews L, Viteri G, Gong C, Lorente P, Fabregat A, Sidiropoulos K, Cook J, Gillespie M, Haw R, et al. The reactome pathway knowledgebase. *Nucleic Acids Res*. 2020;48:D498-d503. doi: 10.1093/nar/gkz1031

25. Fowler ED, Benoist D, Drinkhill MJ, Stones R, Helmes M, Wüst RC, Stienen GJ, Steele DS, White E. Decreased creatine kinase is linked to diastolic dysfunction in rats with right heart failure induced by pulmonary artery hypertension. *J Mol Cell Cardiol*. 2015;86:1-8. doi: 10.1016/j.yjmcc.2015.06.016

26. ter Welle HF, Baartscheer A, Fiolet JW, Schumacher CA. The cytoplasmic free energy of ATP hydrolysis in isolated rod-shaped rat ventricular myocytes. *J Mol Cell Cardiol*. 1988;20:435-441. doi: 10.1016/s0022-2828(88)80135-4

27. Baartscheer A, Schumacher CA, Wüst RC, Fiolet JW, Stienen GJ, Coronel R, Zuurbier CJ. Empagliflozin decreases myocardial cytoplasmic Na(+) through inhibition of the cardiac Na(+)/H(+) exchanger in rats and rabbits. *Diabetologia*. 2017;60:568-573. doi: 10.1007/s00125-016-4134-x

28. Fu X, Wan S, Lyu YL, Liu LF, Qi H. Etoposide induces ATM-dependent mitochondrial biogenesis through AMPK activation. *PLoS One*. 2008;3:e2009. doi: 10.1371/journal.pone.0002009

29. Pan F, Sun L, Kardian DB, Whartenby KA, Pardoll DM, Liu JO. Feedback inhibition of calcineurin and Ras by a dual inhibitory protein Carabin. *Nature*. 2007;445:433-436. doi: 10.1038/nature05476

30. Schickel JN, Pasquali JL, Soley A, Knapp AM, Decossas M, Kern A, Fauny JD, Marcellin L, Korganow AS, Martin T, et al. Carabin deficiency in B cells increases BCR-TLR9 costimulation-induced autoimmunity. *EMBO Mol Med*. 2012;4:1261-1275. doi: 10.1002/emmm.201201595

31. Yang J, Rothermel B, Vega RB, Frey N, McKinsey TA, Olson EN, Bassel-Duby R, Williams RS. Independent signals control expression of the calcineurin inhibitory proteins MCIP1 and MCIP2 in striated muscles. *Circ Res*. 2000;87:E61-68. doi: 10.1161/01.res.87.12.e61

32. Hill JA. Electrical remodeling in cardiac hypertrophy. *Trends Cardiovasc Med*. 2003;13:316-322. doi: 10.1016/j.tcm.2003.08.002

33. Hill JA, Olson EN. Cardiac plasticity. *N Engl J Med*. 2008;358:1370-1380. doi: 10.1056/NEJMra072139

34. Mailleux F, Gélinas R, Beauloye C, Horman S, Bertrand L. O-GlcNAcylation, enemy or ally during cardiac hypertrophy development? *Biochim Biophys Acta*. 2016;1862:2232-2243. doi: 10.1016/j.bbadis.2016.08.012

35. Tran DH, May HI, Li Q, Luo X, Huang J, Zhang G, Niewold E, Wang X, Gillette TG, Deng Y, et al. Chronic activation of hexosamine biosynthesis in the heart triggers

pathological cardiac remodeling. *Nat Commun*. 2020;11:1771. doi: 10.1038/s41467-020-15640-y

36. Tran DH, Wang ZV. Glucose Metabolism in Cardiac Hypertrophy and Heart Failure. *J Am Heart Assoc*. 2019;8:e012673. doi: 10.1161/jaha.119.012673

37. Zhu WZ, Ledee D, Olson AK. Temporal regulation of protein O-GlcNAc levels during pressure-overload cardiac hypertrophy. *Physiol Rep*. 2021;9:e14965. doi: 10.14814/phy2.14965

38. Cabrera-Cruz H, Orostica L, Plaza-Parrochia F, Torres-Pinto I, Romero C, Vega M. The insulin sensitizer mechanism of Myo-inositol is associated to AMPK activation and GLUT-4 expression in human endometrial cells exposed to a PCOS environment. *Am J Physiol Endocrinol Metab*. 2019. doi: 10.1152/ajpendo.00162.2019

39. Zhu WZ, Palazzo T, Zhou M, Ledee D, Olson HM, Paša-Tolić L, Olson AK. First comprehensive identification of cardiac proteins with putative increased O-GlcNAc levels during pressure overload hypertrophy. *PLoS One*. 2022;17:e0276285. doi: 10.1371/journal.pone.0276285

40. Lu S, Liao Z, Lu X, Katschinski DM, Mercola M, Chen J, Heller Brown J, Molkentin JD, Bossuyt J, Bers DM. Hyperglycemia Acutely Increases Cytosolic Reactive Oxygen Species via O-linked GlcNAcylation and CaMKII Activation in Mouse Ventricular Myocytes. *Circ Res*. 2020;126:e80-e96. doi: 10.1161/circresaha.119.316288

41. Hegyi B, Fasoli A, Ko CY, Van BW, Alim CC, Shen EY, Ciccozzi MM, Tapa S, Ripplinger CM, Erickson JR, et al. CaMKII Serine 280 O-GlcNAcylation Links

Diabetic Hyperglycemia to Proarrhythmia. *Circ Res*. 2021;129:98-113. doi: 10.1161/circresaha.120.318402

42. Erickson JR, Pereira L, Wang L, Han G, Ferguson A, Dao K, Copeland RJ, Despa F, Hart GW, Ripplinger CM, et al. Diabetic hyperglycaemia activates CaMKII and arrhythmias by O-linked glycosylation. *Nature*. 2013;502:372-376. doi: 10.1038/nature12537

43. Hegyi B, Borst JM, Bailey LRJ, Shen EY, Lucena AJ, Navedo MF, Bossuyt J, Bers DM. Hyperglycemia regulates cardiac K(+) channels via O-GlcNAc-CaMKII and NOX2-ROS-PKC pathways. *Basic Res Cardiol*. 2020;115:71. doi: 10.1007/s00395-020-00834-8

44. Ramirez-Correa GA, Jin W, Wang Z, Zhong X, Gao WD, Dias WB, Vecoli C, Hart GW, Murphy AM. O-linked GlcNAc modification of cardiac myofilament proteins: a novel regulator of myocardial contractile function. *Circ Res*. 2008;103:1354-1358. doi: 10.1161/circresaha.108.184978

45. Lambert R, Srodulski S, Peng X, Margulies KB, Despa F, Despa S. Intracellular Na+ Concentration ([Na+]i) Is Elevated in Diabetic Hearts Due to Enhanced Na+-Glucose Cotransport. *J Am Heart Assoc*. 2015;4:e002183. doi: 10.1161/jaha.115.002183

46. Facundo HT, Brainard RE, Watson LJ, Ngoh GA, Hamid T, Prabhu SD, Jones SP. O-GlcNAc signaling is essential for NFAT-mediated transcriptional reprogramming during cardiomyocyte hypertrophy. *Am J Physiol Heart Circ Physiol*. 2012;302:H2122-2130. doi: 10.1152/ajpheart.00775.2011

47. Ling SSM, Chen YT, Wang J, Richards AM, Liew OW. Ankyrin Repeat Domain 1 Protein: A Functionally Pleiotropic Protein with Cardiac Biomarker Potential. *Int J Mol Sci*. 2017;18. doi: 10.3390/ijms18071362

48. Piroddi N, Pesce P, Scellini B, Manzini S, Ganzetti GS, Badi I, Menegollo M, Cora V, Tiso S, Cinquetti R, et al. Myocardial overexpression of ANKRD1 causes sinus venosus defects and progressive diastolic dysfunction. *Cardiovascular research*. 2020;116:1458-1472. doi: 10.1093/cvr/cvz291

49. Zhong L, Chiusa M, Cadar AG, Lin A, Samaras S, Davidson JM, Lim CC. Targeted inhibition of ANKRD1 disrupts sarcomeric ERK-GATA4 signal transduction and abrogates phenylephrine-induced cardiomyocyte hypertrophy. *Cardiovascular research*. 2015;106:261-271. doi: 10.1093/cvr/cvv108

50. Murphy NP, Lubbers ER, Mohler PJ. Advancing our understanding of AnkRD1 in cardiac development and disease. *Cardiovascular research*. 2020;116:1402-1404. doi: 10.1093/cvr/cvaa063

51. Maes A, Pestiaux C, Marino A, Balcaen T, Leyssens L, Vangrunderbeeck S, Pyka G, De Borggraeve WM, Bertrand L, Beauloye C, et al. Cryogenic contrast-enhanced microCT enables nondestructive 3D quantitative histopathology of soft biological tissues. *Nat Commun*. 2022;13:6207. doi: 10.1038/s41467-022-34048-4

52. Ripatti S, Tikkanen E, Orho-Melander M, Havulinna AS, Silander K, Sharma A, Guiducci C, Perola M, Jula A, Sinisalo J, et al. A multilocus genetic risk score for coronary heart disease: case-control and prospective cohort analyses. *Lancet*. 2010;376:1393-1400. doi: 10.1016/s0140-6736(10)61267-6

53. Beaney KE, Smith AJP, Folkersen L, Palmen J, Wannamethee SG, Jefferis BJ, Whincup P, Gaunt TR, Casas JP, Ben-Shlomo Y, et al. Functional Analysis of the Coronary Heart Disease Risk Locus on Chromosome 21q22. *Dis Markers*. 2017;2017:1096916. doi: 10.1155/2017/1096916

54. Deidda M, Piras C, Dessalvi CC, Locci E, Barberini L, Torri F, Ascedu F, Atzori L, Mercuro G. Metabolomic approach to profile functional and metabolic changes in heart failure. *J Transl Med*. 2015;13:297. doi: 10.1186/s12967-015-0661-3

55. Santos-Gallego CG, Requena-Ibanez JA, San Antonio R, Ishikawa K, Watanabe S, Picatoste B, Flores E, Garcia-Ropero A, Sanz J, Hajjar RJ, et al. Empagliflozin Ameliorates Adverse Left Ventricular Remodeling in Nondiabetic Heart Failure by Enhancing Myocardial Energetics. *J Am Coll Cardiol*. 2019;73:1931-1944. doi: 10.1016/j.jacc.2019.01.056

56. Di Franco A, Cantini G, Tani A, Coppini R, Zecchi-Orlandini S, Raimondi L, Luconi M, Mannucci E. Sodium-dependent glucose transporters (SGLT) in human ischemic heart: A new potential pharmacological target. *Int J Cardiol*. 2017;243:86-90. doi: 10.1016/j.ijcard.2017.05.032

57. Chen S, Coronel R, Hollmann MW, Weber NC, Zuurbier CJ. Direct cardiac effects of SGLT2 inhibitors. *Cardiovasc Diabetol*. 2022;21:45. doi: 10.1186/s12933-022-01480-1

58. Kasichayanula S, Liu X, Zhang W, Pfister M, Reele SB, Aubry AF, LaCreta FP, Boulton DW. Effect of a high-fat meal on the pharmacokinetics of dapagliflozin, a selective SGLT2 inhibitor, in healthy subjects. *Diabetes Obes Metab*. 2011;13:770-773. doi: 10.1111/j.1463-1326.2011.01397.x

59. Suzuki M, Honda K, Fukazawa M, Ozawa K, Hagita H, Kawai T, Takeda M, Yata T, Kawai M, Fukuzawa T, et al. Tofogliflozin, a potent and highly specific sodium/glucose cotransporter 2 inhibitor, improves glycemic control in diabetic rats and mice. *J Pharmacol Exp Ther*. 2012;341:692-701. doi: 10.1124/jpet.112.191593

## Figures

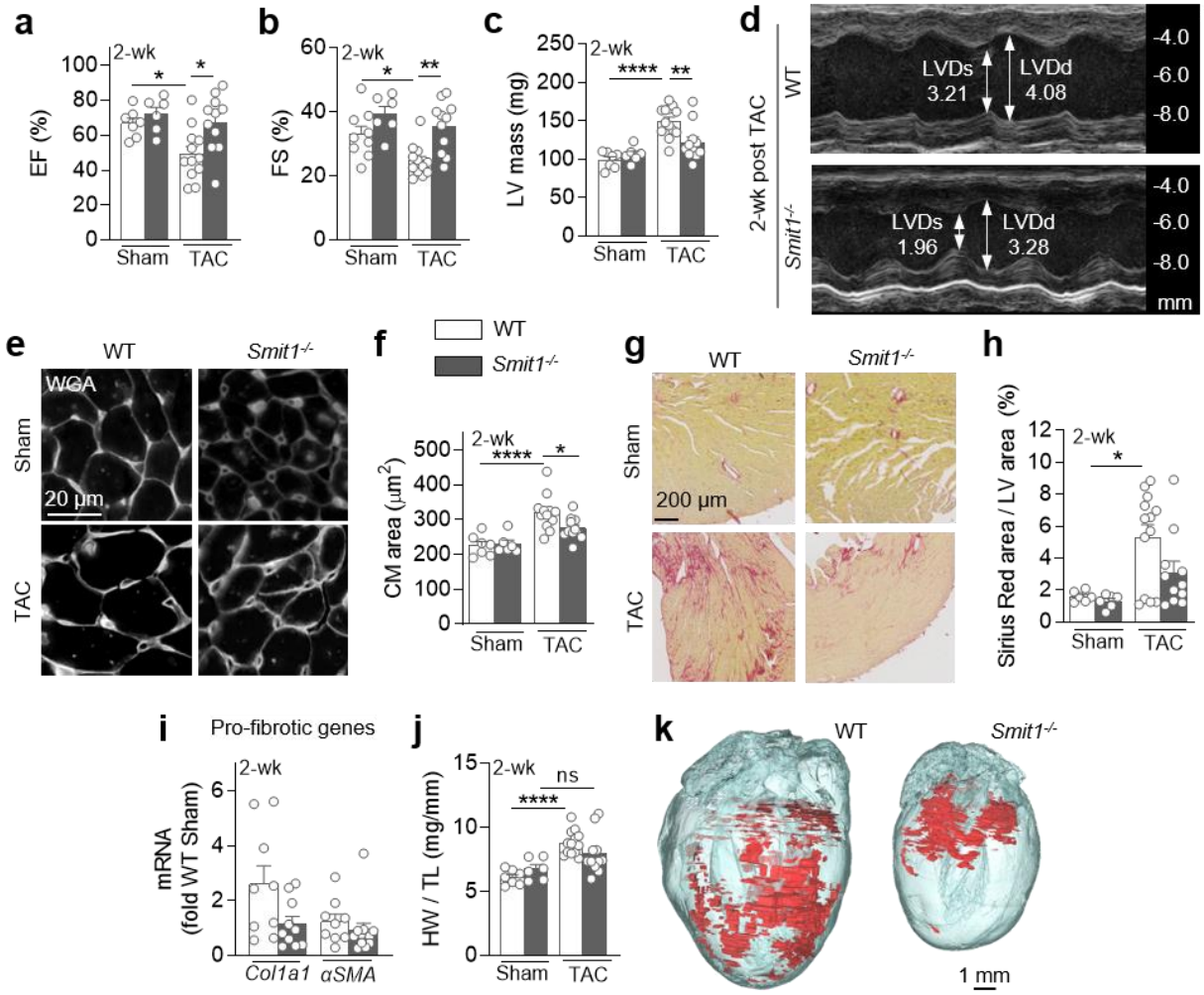


**Figure 1. The absence of SMIT1 prevents the development of cardiac dysfunction, left ventricular hypertrophy and fibrosis during pressure overload.** Echocardiographic analysis of sham- and TAC-operated WT and *Smit1*$^{-/-}$ mice at two weeks after surgery (WT sham n = 7, *Smit1*$^{-/-}$ sham n = 6, WT TAC n = 12, *Smit1*$^{-/-}$ TAC n = 11 animals per group). (**a**) Ejection fraction (EF), (**b**) fractional shortening (FS), and (**c**) left ventricular (LV) mass. (**d**) Representative images of two-dimensional guided M-mode echocardiography of the LV of WT and *Smit1*$^{-/-}$ mice two weeks after TAC. Arrows

indicate the Left-Ventricular End-Diastolic Diameter (LVDd), and the Left-Ventricular End-Systolic Diameter (LVDs). (**e**) Immunofluorescence staining with wheat germ agglutinin (WGA)-rhodamine and (**f**) quantification of cardiomyocytes cross-sectional area from sham control and *Smit1*$^{-/-}$ mice, and mice at two weeks post-TAC. (**g**) Collagen staining with Picrosirius red and (**h**) quantification of cardiac fibrosis in paraffin embedded sections of sham- and TAC-operated mouse hearts. (**i**) RT-qPCR analysis of fibrotic markers on hearts of TAC-operated WT and mutant mice. (**j**) Heart weight/tibia length (HW/TL) ratios of sham- and TAC-operated controls and *Smit1*$^{-/-}$ mice. (**k**) Representative images of heart volume (gray colors) and fibrotic volume (red) 3D rendering of the CECT data of TAC-operated hearts from WT and from *Smit1*$^{-/-}$ mice (n = 3). Data are expressed as mean ± SEM. *P < 0.05, **P < 0.01, ****P < 0.0001. Statistical significance was determined by 2-way ANOVA followed by Tukey's multiple comparison test.

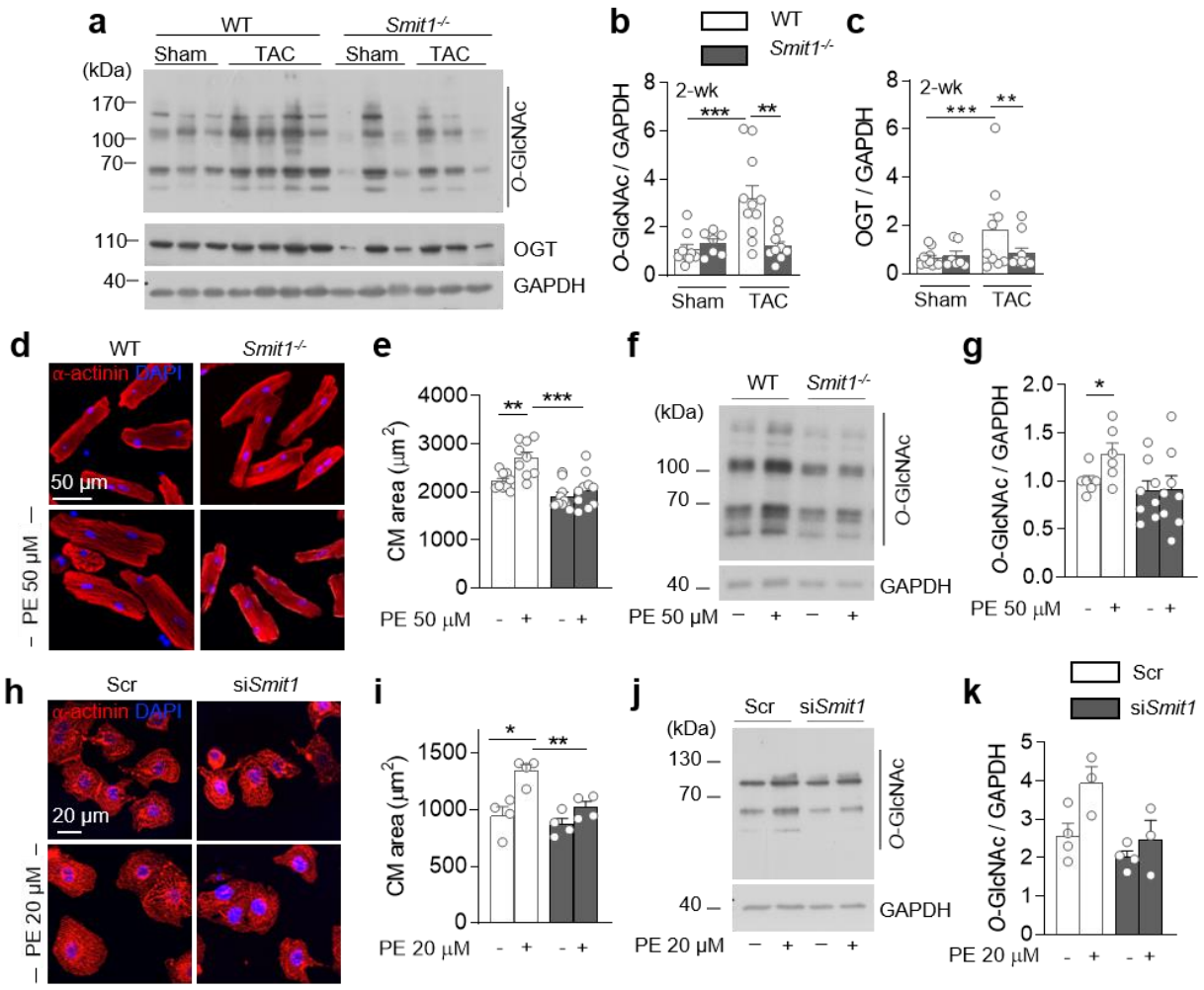


**Figure 2. The absence of SMIT1 protects from hypertrophy through reduced protein *O*-GlcNAcylation *in vivo* and *in vitro*.** (**a**) Representative Western blot and (**b, c**) quantification of total *O*-GlcNAcylation and OGT levels in heart lysates from SMIT1 WT and *Smit1*$^{-/-}$ mice subjected to sham or TAC operation (WT sham n = 9, *Smit1*$^{-/-}$ sham n = 7, WT TAC n = 11, *Smit1*$^{-/-}$ TAC n = 9 animals per group). (**d**) Immunofluorescence analysis and (**e**) quantification of sarcomeric α-actinin (in red) in cultured adult mouse cardiomyocytes (CM) isolated from WT and *Smit1*$^{-/-}$ hearts, treated or not with phenylephrine (PE, 50 µM, 18 hours) (WT n = 9, *Smit1*$^{-/-}$ n = 10 isolations per group). (**f**)

Western blot analysis and (**g**) quantification of total *O*-GlcNAcylation levels in PE-treated WT and *Smit1*$^{-/-}$ cardiomyocytes. Nuclei were counterstained with DAPI (in blue). (**h**) Immunofluorescence analysis and (**i**) quantification of sarcomeric α-actinin (in red) of neonatal rat cardiomyocytes (CM) transfected with Scramble (Scr) or SMIT1 siRNA treated with or without PE (20 µM, 48 h) (n = 4 isolations per group). Nuclei were counterstained with DAPI (in blue). (**j**) Western blot analysis and (**k**) quantification of total *O*-GlcNAcylation in PE-treated neonatal rat cardiomyocytes transfected wit Scr or si*Smit1*. GAPDH was used as loading control. *P<0.05, **P<0.01, ***P<0.001 by 2-way ANOVA followed by Tukey's multiple comparison test.

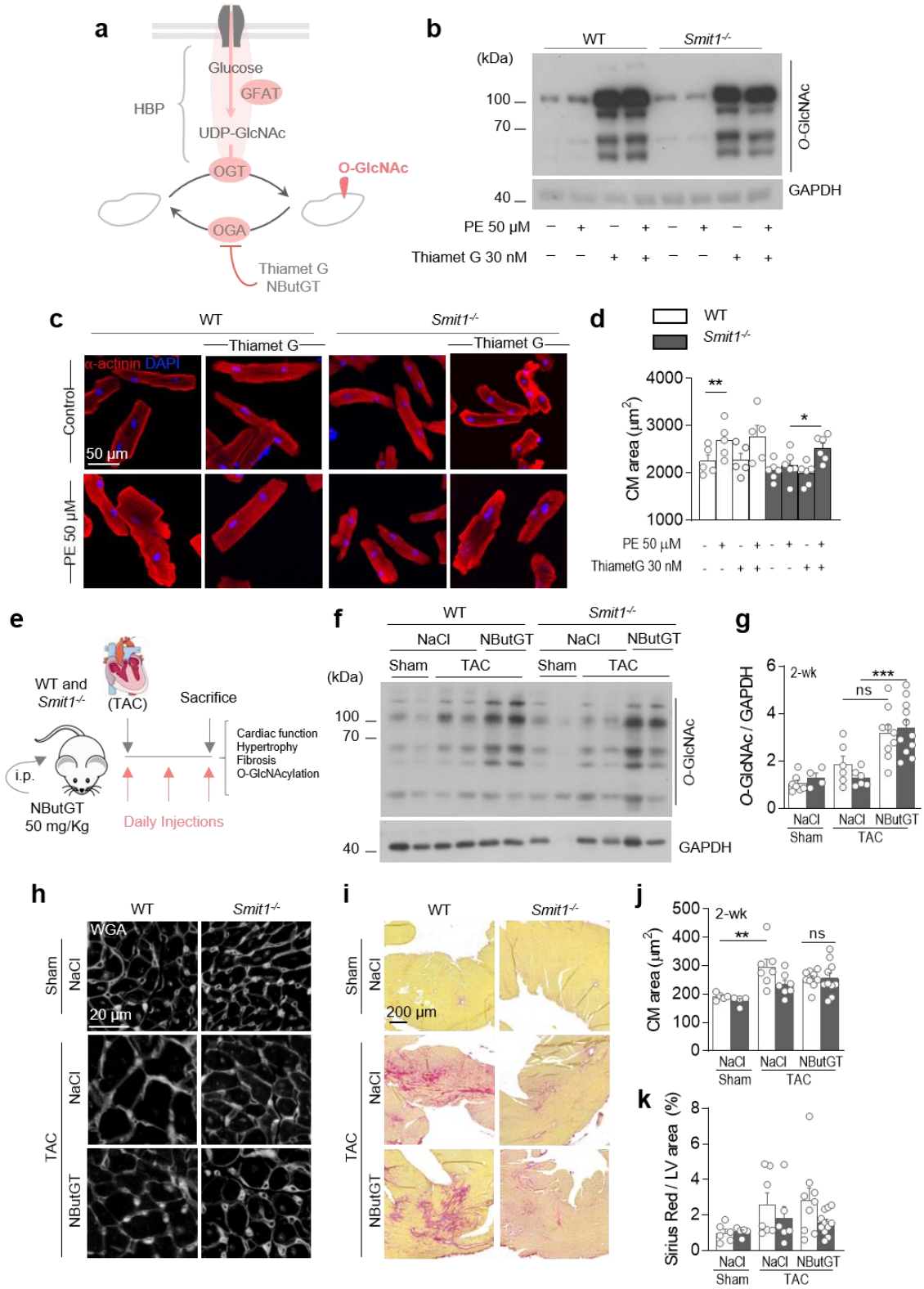
a
Glucose
GFAT
HBP
UDP-GlcNAc
OGT
O-GlcNAc
OGA
Thiamet G
NButGT
b
WT
Smit1-/-
(kDa)
100
70
40
O-GlcNAc
GAPDH
PE 50 μM
Thiamet G 30 nM
c
WT
Smit1-/-
Thiamet G
α-actinin DAPI
Control
PE 50 μM
50 μm
d
WT
Smit1-/-
CM area (μm2)
4000
3000
2000
1000
**
*
PE 50 μM
ThiametG 30 nM
e
WT and Smit1-/-
(TAC)
Sacrifice
i.p.
NButGT
50 mg/Kg
Daily Injections
Cardiac function
Hypertrophy
Fibrosis
O-GlcNAcylation
f
WT
Smit1-/-
NaCl
NButGT
Sham
TAC
(kDa)
100
70
40
O-GlcNAc
GAPDH
g
O-GlcNAc / GAPDH
2-wk
***
ns
NaCl
NaCl
NButGT
Sham
TAC
h
WT
Smit1-/-
WGA
Sham
NaCl
TAC
NaCl
NButGT
20 μm
i
WT
Smit1-/-
Sham
NaCl
TAC
NaCl
NButGT
200 μm
j
CM area (μm2)
2-wk
**
ns
NaCl
NaCl
NButGT
Sham
TAC
k
Sirius Red / LV area (%)
NaCl
NaCl
NButGT
Sham
TAC

**Figure 3. Pharmacological induction of *O*-GlcNAcylation blocks the anti-hypertrophic effect observed in the absence of SMIT1.** (**a**) Schematic of the *O*-GlcNAcylation pathway. GFAT: glutamine-fructose-6-phosphate transaminase 1, OGT: *O*-GlcNAc transferase, OGA: *O*-GlcNAcase. (**b**) Representative *O*-GlcNAc Western blot, (**c**) α-actinin immunostaining (in red) and (**d**) quantification of the area of WT and *Smit1*$^{-/-}$ isolated cardiomyocytes (CM) treated or not with phenylephrine (PE, 50 µM) (WT n = 5, *Smit1*$^{-/-}$ n = 6 isolations per group). Nuclei were counterstained with DAPI (in blue). (**e**) Experimental scheme of NButGT treatment of TAC-operated WT and *Smit1*$^{-/-}$ mice. (**f,g**) Western blot analysis of *O*-GlcNAc levels and immunofluorescence analysis of paraffin embedded hearts stained for (**h**) WGA and (**i**) Picrosirius red, with respective quantification (**j**,**k**) (WT sham n = 5, *Smit1*$^{-/-}$ sham n = 4, WT TAC NaCl n = 7, *Smit1*$^{-/-}$ TAC NaCl n = 7, WT TAC NButGT n = 10, *Smit1*$^{-/-}$ TAC NButGT n = 11 animals per group).

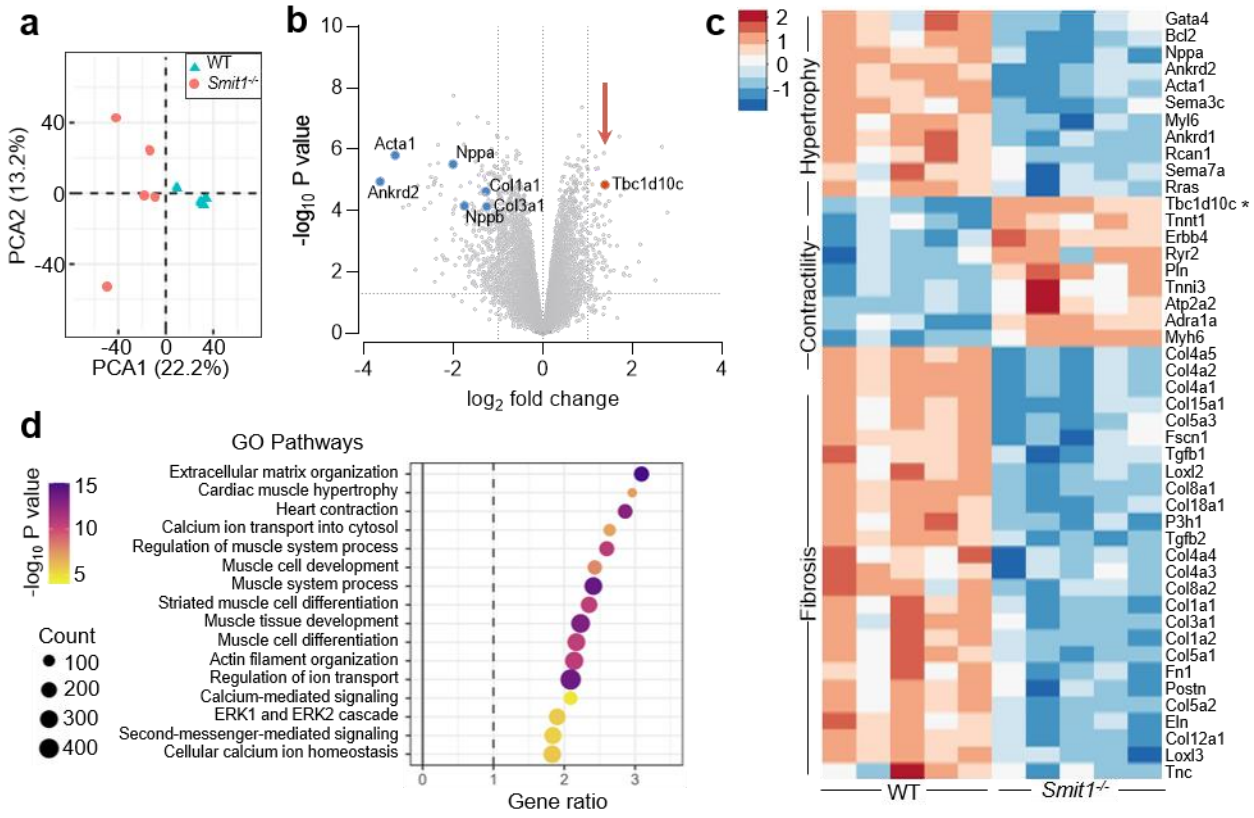


**Figure 4. The absence of SMIT1 induces significant changes in gene expression in murine hearts after TAC, including calcium signaling.** (**a**) Principal component analysis (PCA) of WT and *Smit1*$^{-/-}$ hearts at two weeks post TAC (n = 5 animals per group). Volcano plot representation of differentially expressed genes in WT and *Smit1*$^{-/-}$ hearts at two weeks post TAC (n = 5 animals per group), highlighting upregulation of *Tbc1d10c* gene (Carabin), and downregulation of hypertrophic and fibrotic genes (*Acta1*, *Nppa*, *Nppb*, Ankrd2, *Col1a1, Col3a1*). (**b**) Heat maps showing changes in gene expression of cardiac hypertrophy, fibrosis, and contractility in TAC-operated WT vs *Smit1*$^{-/-}$ hearts. (**c**) Enrichment ratios obtained from the over-representation analysis (ORA). The selection of significant terms shown here belongs to the biological process (BP) gene ontology (GO). The dot diameter is proportional to the total number of genes in the GO pathway and the color indicates the enrichment P-value.

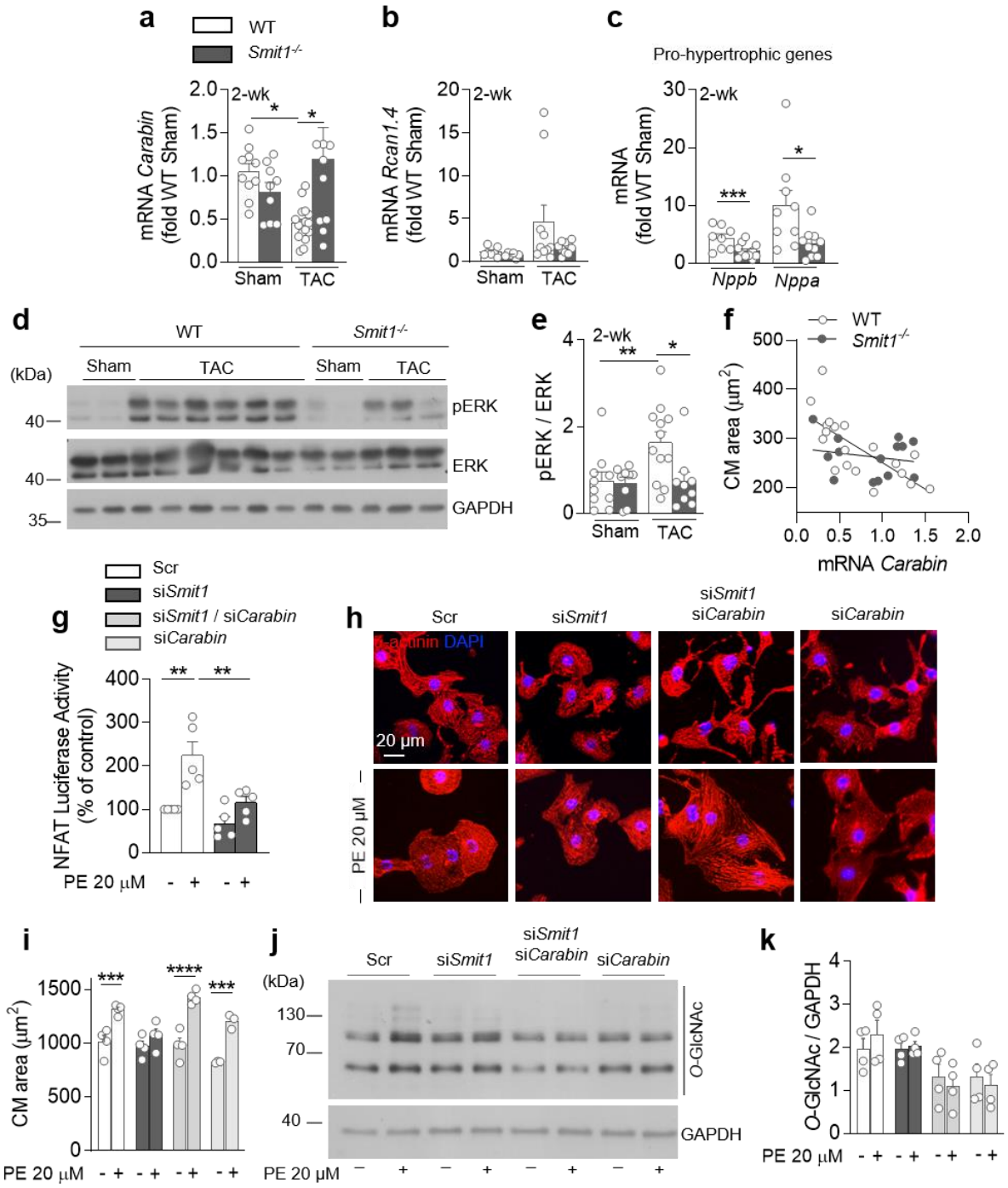


**Figure 5. SMIT1 modulates the pro-hypertrophic pathways via Carabin.** (**a**) Carabin and (**b**) *Rcan1.4* (calcineurin activity) in mouse hearts from WT and *Smit1*$^{-/-}$ mice at two weeks post TAC. (**c**) mRNA levels of pro-hypertrophic genes (*Nppb*, *Nppa*) two weeks after surgery in TAC-operated WT and *Smit1*$^{-/-}$ mouse hearts. (**d**) Representative Western

blot and (**e**) quantification of total and phosphorylated ERK1/2 in sham- and TAC-operated WT and *Smit1*$^{-/-}$ (WT sham n ≥ 7, *Smit1*$^{-/-}$ sham n ≥ 6, WT TAC n ≥ 10, *Smit1*$^{-/-}$ TAC n ≥ 10 animals per group). (**f**) Correlation between cardiomyocyte (CM) area and Carabin mRNA levels. (**g**) NFAT-Luciferase activity measured in neonatal rat cardiomyocytes transfected with Scr or si*Smit1* treated with or without PE 20 µM (n = 5 isolations per groups). (**h**) Representative immunofluorescence images and (**i**) area quantification of α-actinin stained neonatal rat cardiomyocyte transfected with Scr, si*Smit1*, si*Smit1* + si*Carabin*, and si*Carabin* treated with or without PE 20 µM for 24 hours. Nuclei were counterstained with DAPI (in blue). (**j**) Western blot and (**k**) quantification representing *O*-GlcNAcylated proteins and loading control (GAPDH) in neonatal rat cardiomyocytes transfected with Scr, si*Smit1*, si*Smit1* + si*Carabin*, and si*Carabin* (n = 4 isolations per groups). *P<0.05, **P<0.01, ***P<0.001 by 2-way ANOVA followed by Tukey's multiple comparison test.

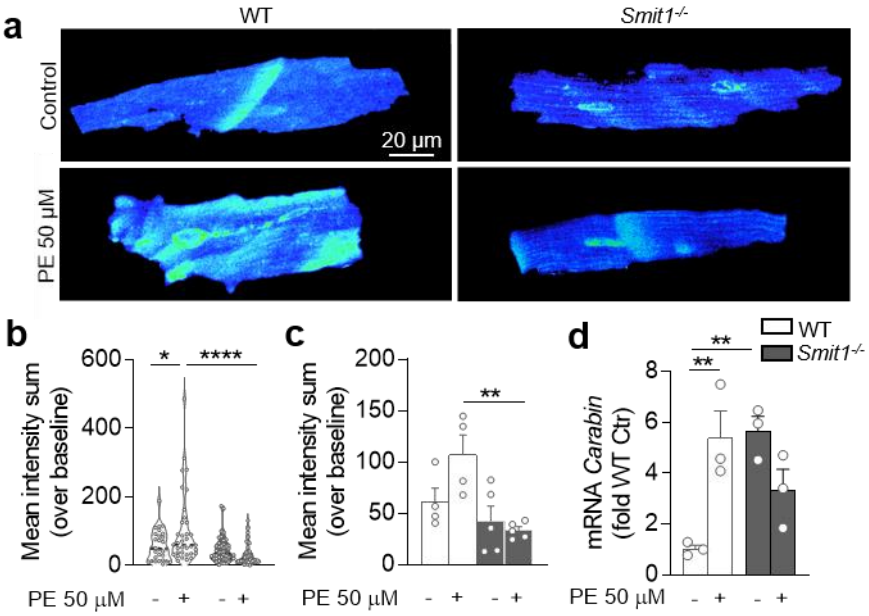


**Figure 6. The absence of SMIT1 attenuates PE-induced calcium fluxes in cardiomyocytes**. (**a**) Representative images of fluorescence recording of Fluo-4 loaded living cardiomyocytes from adult WT and *Smit1*$^{-/-}$ mice treated with or without PE (50 µM). Mean intensity fluorescence over time measured in (**b**) each cardiomyocyte (WT control n = 29, WT PE n = 35, *Smit1*$^{-/-}$ control n = 43, *Smit1*$^{-/-}$ PE n = 45) and (**c**) averaged per experiment (WT n = 4, *Smit1*$^{-/-}$ n = 5). (**d**) Carabin mRNA levels measured in cardiomyocytes from adult WT and *Smit1*$^{-/-}$ mice treated with or without PE (50 µM, 18 h, n = 3). *P<0.05, **P<0.01, ****P<0.0001 by 2-way ANOVA followed by Tukey's multiple comparison test.

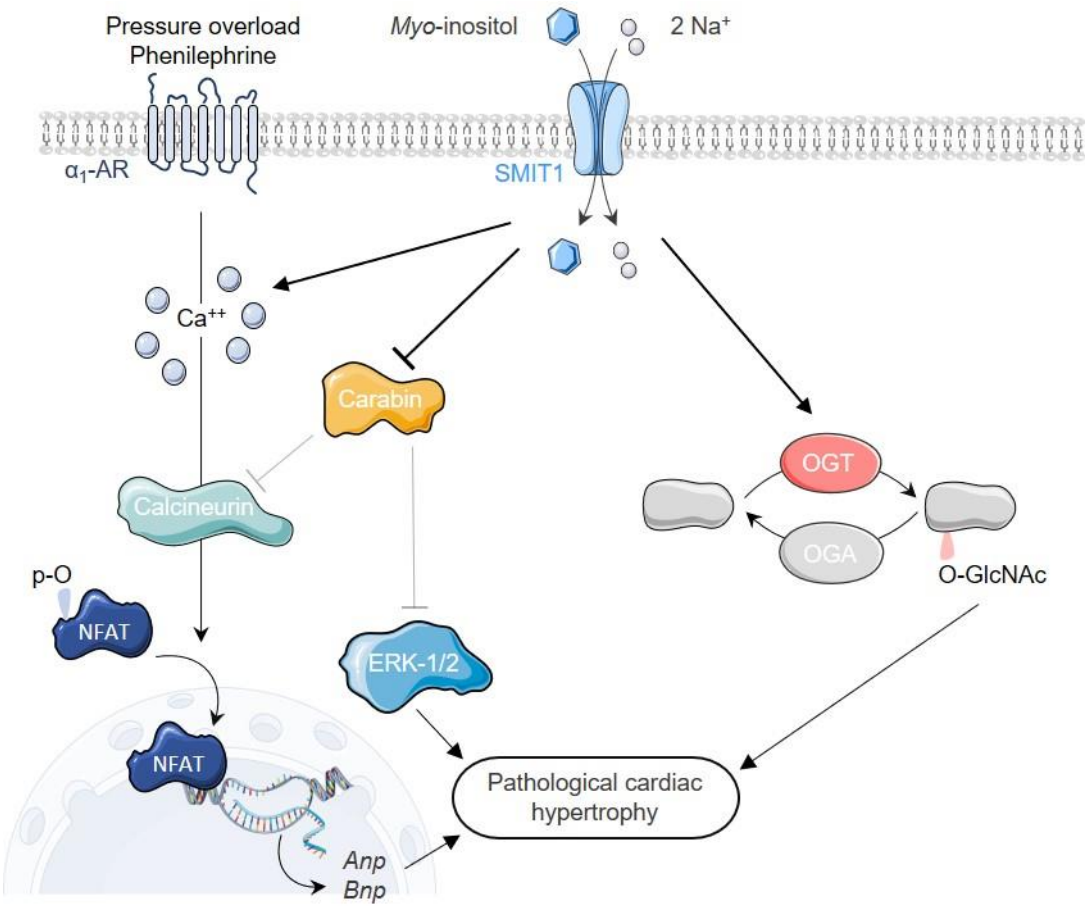


**Graphical abstract. Model of the role of SMIT1 in the development of cardiac hypertrophy.** We found that SMIT1 modulates intracellular calcium levels, downregulates Carabin and increases OGT expression, to promote pathological cardiac hypertrophy and heart failure development.